AGU PUBLICATIONS

Space Weather

INTRODUCTION TO SPECIAL SECTION

10.1002/2016SW001399

Special Section:
Initial Results from the NASA Radiation Dosimetry Experiment (RaD-X) Balloon Flight Mission

Key Points:
- Flight measurements were taken to improve aviation radiation models
- Benchmark dosimetric measurements at seven altitudes were obtained to characterize cosmic ray primary and secondary radiations
- The science background and motivation for the flight campaign are given

Correspondence to:
C. J. Mertens,
Christopher.J.Mertens@nasa.gov

Citation:
Mertens, C. J. (2016), Overview of the Radiation Dosimetry Experiment (RaD-X) flight mission, *Space Weather*, *14*, 921–934, doi:10.1002/2016SW001399.

Received 19 APR 2016
Accepted 16 OCT 2016
Accepted article online 25 OCT 2016
Published online 9 NOV 2016

Overview of the Radiation Dosimetry Experiment (RaD-X) flight mission

Christopher J. Mertens[1]

[1] NASA Langley Research Center, Hampton, Virginia, USA

Abstract The NASA Radiation Dosimetry Experiment (RaD-X) stratospheric balloon flight mission addresses the need to reduce the uncertainty in predicting human exposure to cosmic radiation in the aircraft environment. Measurements were taken that characterize the dosimetric properties of cosmic ray primaries, the ultimate source of aviation radiation exposure, and the cosmic ray secondary radiations that are produced and transported to aviation altitudes. In addition, radiation detectors were flown to assess their potential application to long-term, continuous monitoring of the aircraft radiation environment. RaD-X was successfully launched from Fort Sumner, New Mexico (34.5°N, 104.2°W), on 25 September 2015. Over 18 h of science data were obtained from a total of four different type dosimeters at altitudes above 20 km. The RaD-X flight mission was supported by laboratory radiation exposure testing of the balloon flight dosimeters and also by coordinated radiation measurements taken on ER-2 and commercial aircraft. This paper provides the science background and motivation for the RaD-X flight mission, a brief description of the balloon flight profile and the supporting aircraft flights, and a summary of the articles included in the RaD-X special collection and their contributions to the science goals of the RaD-X mission.

1. Background and Motivation

Energetic particle radiation from space continuously bombards the Earth's atmosphere. Cosmic radiation has sufficient energy to penetrate deep within the atmosphere and adversely affect human health to crew and passengers on aircraft [*Reitz*, 1993; *Dachev*, 2013]. There are two sources of cosmic rays: (1) the ever-present galactic cosmic rays (GCR), with origins outside the solar system and (2) the transient solar energetic particles (SEP) (or solar cosmic rays), which are associated with eruptions on the Sun's surface lasting several hours to days.

Cosmic radiation is effective at directly breaking deoxyribonucleic acid strands in biological tissue or producing chemically active radicals in tissue that alter the cell function, both of which can lead to adverse health effects [*Wilson et al.*, 2003, 2005]. For example, studies of female flight attendants have suggested adverse reproductive outcomes [*Aspholm et al.*, 1999; *Lauria et al.*, 2006; *Waters et al.*, 2000]. Also, a recent epidemiological study has shown a 70% increase in the risk of miscarriage among flight attendants who received a dose of 0.1 mGy (1 Gy = J/kg) or more in their first trimester [*Grajewski et al.*, 2015].

The International Commission on Radiological Protection (ICRP) classifies crews of commercial aircraft as radiation workers [*International Commission on Radiological Protection* (*ICRP*), 1991, 2007]. Commercial aircrew are among the highest occupationally exposed workers in the terrestrial environment [*United Nations Scientific Committee on the Effects of Atomic Radiation* (*UNSCEAR*), 2000]. The United States (U.S.) National Council on Radiation Protection and Measurements (NCRP) reported that among terrestrial radiation workers monitored during the period between 2003 and 2006, the largest average effective dose was found in flight crews, who received an average annual dose of roughly 3 mSv [*United Nations Scientific Committee on the Effects of Atomic Radiation*, 2000; *National Council on Radiation Protection and Measurements*, 2009]. This is nearly double the average annual radiation exposure from natural background sources for a person living in the U.S. [*National Council on Radiation Protection and Measurements*, 2009]. A survey of radiation exposure to Air Canada pilots during the recent solar minimum showed that the majority of pilots received more than 1 mSv per annum [*Bennett et al.*, 2013]. This radiation level would require individual exposure assessment in some countries [*Lindborg et al.*, 2004]. The majority of pilots in the Air Canada study received around 3 mSv, consistent with the

previous studies [*United Nations Scientific Committee on the Effects of Atomic Radiation*, 2000; *National Council on Radiation Protection and Measurements*, 2009], but with a few pilots receiving near 5 mSv [*Bennett et al.*, 2013].

For commercial aircrew in the European Union (EU), work schedules are arranged to keep annual exposures below 6 mSv. If an annual exposure exceeds 6 mSv, individual medical surveillance and record keeping is recommended, according to a Directive issued by the Commission of the European Communities [*EURATOM*, 1996]. The ICRP recommended exposure limit for a nonpregnant, radiation worker is a 5 year average of 20 mSv yr, with no more than 50 mSv in a single year [*International Commission on Radiological Protection (ICRP)*, 1991, 2007]. The 6 mSv action level for EU aircrew is an implementation of as low as reasonably achievable principle of radiation protection. However, in most countries, including the U.S., aircrews are the only occupational group exposed to unquantified and undocumented radiation levels over the duration of their careers.

The ICRP 1 mSv limit for public and prenatal planned exposure situations [*International Commission on Radiological Protection (ICRP)*, 2007], such as air flights, can be exceeded during a single solar storm event for passengers on commercial intercontinental or cross-polar routes, or by frequent use (~5–10 round-trip flights per year) of these high-latitude routes even in the absence of solar storms [*AMS*, 2007; *Copeland et al.*, 2008; *Dyer et al.*, 2009; *Mertens et al.*, 2012]. For the typical range of high-latitude GCR effective dose rates at commercial aviation altitudes [*Lindborg et al.*, 2004; *Mertens et al.*, 2013], ~5–10 μSv/h, a 10 h flight incurs an effective dose of ~0.05–0.1 mSv. Thus, 5–10 round-trip high-latitude flights per year can exceeded the ICRP public or prenatal limit. A chest X-ray is equivalent to a radiation exposure of 0.1 mSv [*International Commission on Radiological Protection (ICRP)*, 1991]. Therefore, one receives the equivalent of 1–2 chest X-rays on a round-trip, high-latitude commercial air flight. On average, the 100,000 mile flyer receives 2 mSv, or 20 chest X-rays (estimate based on results reported by *Mertens et al.* [2013]).

Copeland et al. [2008] calculated aviation radiation exposure for 170 SEP events from 1986 to 2008. The NCRP recommended conceptus exposure limit of 0.5 mSv per month was exceeded during 10 of these solar storm events [*Friedberg and Copeland*, 2011]. The highest exposures acquired were during the 29 September 1989 and 20 January 2005 events, reaching nearly 1 mSv for a 10 h commercial flight at high latitudes. *Dyer et al.* [2003] estimated 1–3 mSv exposure for high-latitude commercial flights during the 23 February 1956 event.

Thus, there is a recognized need to link scientific knowledge of atmospheric cosmic radiation impacts to aviation decision making with respect to aircrew and passenger exposure [*Fisher*, 2009]. The need and conceptual requirements for atmospheric cosmic radiation forecast models during SEP events were discussed by *Kataoka et al.* [2011]. *Stassinopoulos et al.* [2003] and *Tobiska et al.* [2015] emphasized the need for global monitoring of the atmospheric cosmic radiation environment in order to improve the performance of aviation radiation exposure models. The transport of cosmic radiation into the atmosphere is susceptible to spatial-temporal variability associated with complex interplanetary and magnetospheric processes, such as Forbush decreases and geomagnetic storms, both of which are not well represented in current models [*Spurný et al.*, 2004; *Getley*, 2004; *Getley et al.*, 2005].

A significant step forward in quantifying and documenting aircraft radiation exposure has been made via the development of NASA's Nowcast of Atmospheric Ionizing Radiation for Aviation Safety (NAIRAS) model. NAIRAS is the first real-time, global, physics-based aviation radiation model which includes both GCR and SEP sources of atmospheric cosmic radiation [*Mertens et al.*, 2012, 2013]. It also incorporates the dynamical response of the geomagnetic field to variations in the interplanetary medium [*Kress et al.*, 2010; *Mertens et al.*, 2010]. It is a free-running physics-based model in the sense that no adjustment factors are applied to nudge the model into agreement with measurement data. NAIRAS real-time graphical and tabular products are streaming live from the project's public web site at http://sol.spacenvironment.net/~nairas/ (or, conduct an internet search for NAIRAS).

The NAIRAS model is composed of coupled physics-based models that transport cosmic radiation through the heliosphere, Earth's magnetosphere, and neutral atmosphere. The energy spectrum of cosmic radiation incident at the top of the atmosphere has been altered by interactions with the interplanetary magnetic field, carried by the solar wind and the Earth's magnetic field environment [*Mertens et al.*, 2013]. Further penetration into the atmosphere results in continuous energy loss of cosmic ray particles via ionization of the surrounding

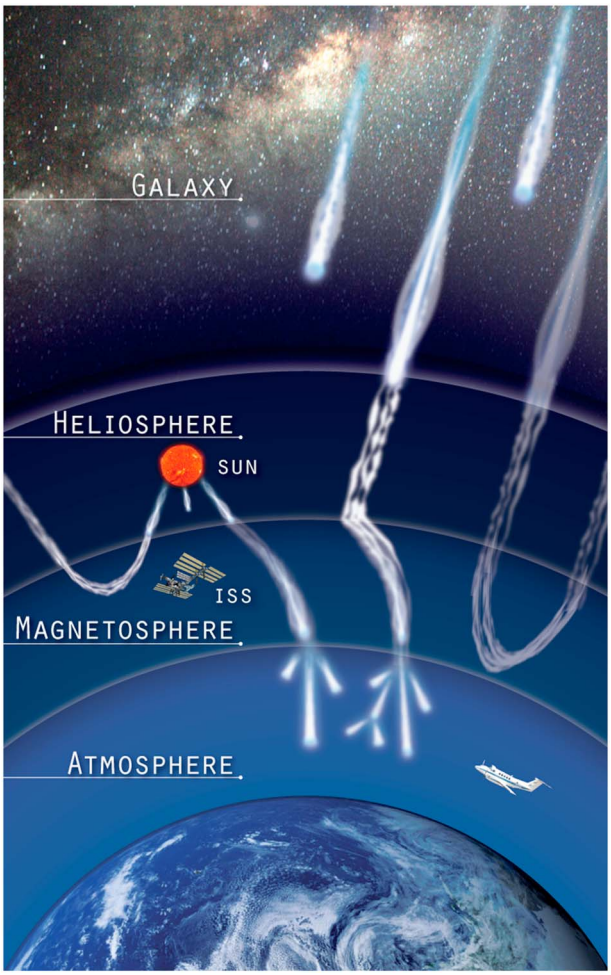

Figure 1. An artistic depiction of the interaction and transport of cosmic rays through the heliosphere and Earth's magnetic environment and neutral atmosphere.

atmosphere. Moreover, collisions between cosmic radiation and the atmospheric constituents can generate secondary radiation through nuclear fragmentation processes [*Mertens et al.*, 2012]. An artistic depiction of this broad category of processes is shown in Figure 1.

The NAIRAS model computes cosmic ray particle flux spectra, including neutrons and other nucleonic secondary radiations produced from nuclear interactions between cosmic ray primary particles and the atmospheric constituents [*Wilson et al.*, 1991]. The spectral fluxes are the fundamental physical quantities from which other useful quantities can be derived. For example, the model calculates the dosimetric quantities that are important for radiation protection applications and other dosimetric and spectroscopic quantities that can be compared directly to measurement data to facilitate model verification and validation (V&V) [*Mertens et al.*, 2012, 2013].

A primary dosimetric quantity used in radiation protection is effective body dose [*International Commission on Radiological Protection (ICRP)*, 1991], a quantity related to biological risk. However, effective dose is not a practical quantity to measure. Therefore, the *International Commission on Radiological Protection (ICRP)* [1991] has recommended the use of ambient dose equivalent as an operational radiation protection quantity, which can be obtained from microdosimeter measurements combined with certain calibration factors [*Lillhök et al.*, 2007; *Silari et al.*, 2009]. Thus, ambient dose equivalent provides a reasonable measurement proxy for effective body dose [*International Commission on Radiological Protection (ICRP)*, 2007; *ICRU*, 2010; *Meier et al.*, 2009]. A brief description of these dosimetric quantities and the quantities measured by the RaD-X science instruments are given in section 3.

The dosimetric quantities and energy deposition spectral quantities computed by the NAIRAS model are summarized as follows. The model computes effective dose rate so that the end users can use this quantity for radiation risk assessment and radiation exposure management and mitigation. The model also calculates the ambient dose equivalent rate for direct comparison to microdosimeter measurements. Energy deposition spectra in tissue and silicon are also calculated, as well as absorbed dose rate in silicon, in order to facilitate V&V by providing model output quantities that can be directly compared to silicon-based dosimeters and spectrometers.

The NAIRAS model predictions of ambient dose equivalent rates were compared with GCR aircraft measurements [*Mertens et al.*, 2013]. The measurement sources were the reference data tabulated by the International Commission on Radiation Units and Measurements (ICRU) [*ICRU*, 2010], and the onboard aircraft radiation measurements taken by the German Aerospace Center (Deutsches Zentrum für Luft- und Raumfahrt, DLR) in 2008 [*Hubiak*, 2008; *Meier et al.*, 2009]. The ICRU reference measurements covered the typical range of commercial aircraft cruising altitudes and the full range of geomagnetic vertical cutoff rigidities and the extrema of solar cycle activity levels. The DLR flight measurements used in the NAIRAS model comparisons covered the full range of vertical cutoff rigidities at commercial flight levels during the deep minimum between solar cycle 23 and solar cycle 24. The NAIRAS ambient dose equivalent rate predictions were generally within 10% of the flight measurements at high latitudes [*Mertens et al.*, 2013]. The NAIRAS model systematically underpredicted ambient dose equivalent rates measured at midlatitude to low latitude, where the vertical cutoff rigidity increases with decreasing latitude toward the equator, with differences exceeding 50% [*Mertens et al.*, 2013].

The comparisons of the NAIRAS model to the radiation measurements reported by *Mertens et al.* [2013] provided an assessment of the model predictions at commercial aircraft cruising altitudes. However, comparisons to aircraft radiation measurements alone are insufficient to fully characterize model performance and unambiguously identify its primary sources of uncertainty. The composition and energy spectrum of cosmic radiation change as a function of depth within the atmosphere [*Reitz*, 1993; *Ferrari et al.*, 1999; *Copeland*, 2014], while commercial aircraft cruising altitudes correspond to roughly the same pressure level or depth within the atmosphere. Consequently, radiation measurements covering a wide range of altitudes are required to fully assess aviation radiation models. This point is expounded below.

GCR consist of roughly 90% protons and 8% helium nuclei with the remainder being heavier nuclei and electrons [e.g, *Gaisser*, 1990]. Collisions between these high-energy cosmic ray primaries and the atmospheric constituents produce secondary particles, as mentioned previously, which can cascade into additional showers of particles. A simplified schematic of an atmospheric shower event is shown in Figure 2. A collision between a cosmic ray primary particle and an atmospheric atom produces mainly secondary protons, neutrons, and pions [*Gaisser*, 1990; *Reitz*, 1993]. The charged pions decay into muons and neutrinos. The muons subsequently decay into electrons, positrons, and neutrinos. The neutral pion decays into high-energy photons, which can create electron-positron pairs. The production of particles through the pion-initiated processes is referred to as the electromagnetic cascade. The secondary protons and neutrons can produce additional nucleons through subsequent collision events. This category of processes is referred to as the nucleon cascade. Secondary particle production continues to increase with depth in the atmosphere until a peak in the cosmic radiation flux is reached. The flux monotonically decreases at depths greater than the depth of the peak flux.

The peak in the charged particle component of atmospheric cosmic radiation flux is known as the Pfotzer maximum [*Reitz*, 1993]. The Pfotzer maximum varies with latitude (more precisely, geomagnetic vertical cutoff rigidity) and solar cycle activity and is generally located at 15–27 km [*Bazilevskaya and Svirzhevskaya*, 1998; *Bazilevskaya*, 2000; *Singh et al.*, 2011]. Figure 3 shows balloon measurements of atmospheric ionization rates at various latitudes during solar cycle minimum [*Neher*, 1967]. The Pfotzer maximum corresponds roughly to the peak in the production of secondary radiation. There are virtually no remaining cosmic ray heavy-ion primaries ($Z > 2$) below about 30 km. At this altitude, the high-energy heavy ions have collided with the atmospheric constituents, producing showers of secondary particles, or the lower energy heavy ions have been stopped through ionization energy loss and charge neutralization [*Mertens et al.*, 2012]. In the region just above the Pfotzer maximum (~20–27 km), protons are the remaining cosmic ray primary particles. Below the Pfotzer maximum, atmospheric cosmic radiation is comprised almost entirely of secondary radiation. The relative contribution of the secondary particles to the total cosmic radiation flux and energy deposition rate varies

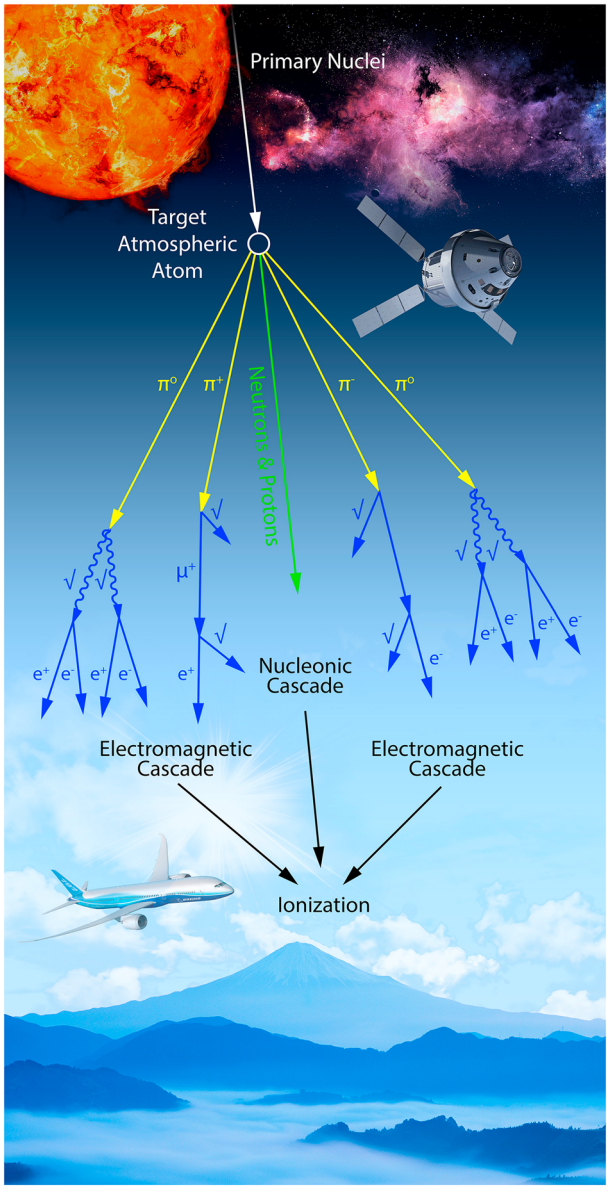

Figure 2. Schematic of categories of particle production in secondary atmospheric cosmic radiation.

with depth in the atmosphere, latitude (i.e., geomagnetic vertical cutoff rigidity), and solar cycle activity [*Reitz*, 1993; *Ferrari et al.*, 1999; *Copeland*, 2014]. Commercial aircraft cruising altitudes are at 10–12 km, which is below the Pfotzer maximum. Thus, aviation radiation exposure is attributed almost exclusively to secondary cosmic ray particles.

Based on the above discussion, the difficulties of aviation radiation model development and validation are evident. A physics-based model must accurately predict the cosmic ray primary particles incident at the top of the atmosphere and the subsequent secondary particle production interactions and transport processes at all altitudes above commercial flight levels, in order to yield accurate radiation exposure predictions at aviation altitudes. Furthermore, radiation measurements covering a range of atmospheric altitudes, latitudes, and solar cycle activity are required to fully assess and validate physics-based aviation radiation models.

Stratospheric research balloons provide an important platform for collecting cosmic radiation measurements for aviation radiation model assessment and validation. The balloon platform enables an observational characterization of cosmic radiation primary particles, as discussed above. Additionally, the natural diurnal variation in the balloon's float altitude can be utilized to provide measurements in a region where energy

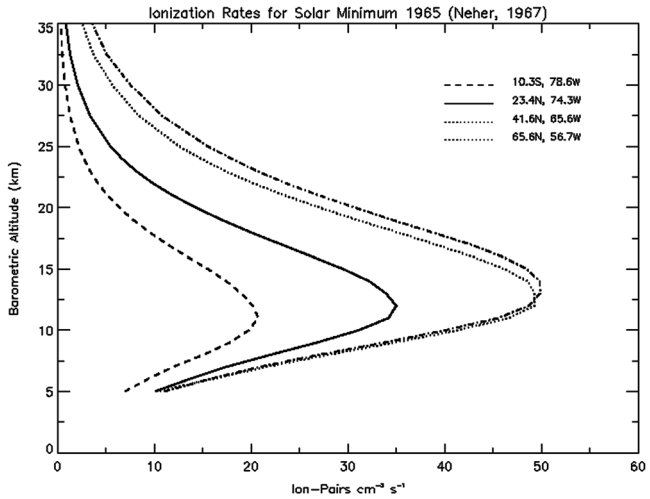

Figure 3. Balloon measurements of atmospheric ionizing rates at solar cycle minimum. The latitude (degrees) and longitude (degrees) of the measurements are indicated in the legend.

deposition from heavy-ion cosmic ray primaries are clearly discernable and measurements at altitudes just above the Pfotzer maximum where protons are nearly the sole source of cosmic ray primary particles depositing energy. Thus, stratospheric balloons provide a platform amenable to the characterization of the sources of cosmic radiation exposure at aviation altitudes. Furthermore, unlike commercial aircraft flight trajectories, the high-altitude balloon trajectory can be confined to a narrow range in vertical cutoff rigidity for at least 24 h of science data collection, depending on the location of the launch site. This provides long-duration measurements at a nearly constant geomagnetic vertical cutoff rigidity, permitting a significant reduction in the statistical variation in the balloon flight radiation measurements.

2. The RaD-X Flight Campaign

The above discussion provides the background context and motivation for the NASA Radiation Dosimetry Experiment (RaD-X) flight mission, which is the focus of this special issue of space weather. RaD-X addresses the need to reduce the uncertainty in the prediction of human exposure to cosmic radiation in the aircraft environment by identifying two primary science goals for improving the assessment of aviation radiation exposure. The first goal is to provide measurements that will characterize the dosimetric properties of cosmic ray primaries, which are the ultimate source of aviation radiation exposure. These measurements will enable aviation radiation models, such as the NAIRAS model discussed above, to evaluate the contribution of uncertainty in predicting cosmic ray primaries and the subsequent propagation of this uncertainty into the prediction of radiation exposure at aircraft altitudes. The second science goal is to identify and characterize low-cost, compact radiation measurement technologies. Long-term, continuous monitoring of the aircraft radiation environment is needed to improve the accuracy and reliability of real-time, global radiation model predictions, especially during SEP events when decisions about radiation health risk and the potential adjustments to flight routes need to be made. Achieving this goal requires the development of cost-effective radiation detectors that can be distributed on airline fleets.

Progress toward achieving the RaD-X science mission goals was made with the RaD-X stratospheric balloon flight, which was launched from Fort Sumner, New Mexico (34.5°N, 104.2°W), on 25 September 2015. The balloon flight data contained over 18 h of science data in two primary altitude regimes: (1) above 32 km (average flight pressure was 4.5 hPa), where the presence of heavy-ion cosmic primaries are discernable in some of the dosimetric measurements, and (2) between 21 and 27 km (average flight pressure was 27.3 hPa), where protons are almost exclusively the source of cosmic ray primary particle contributions to the dosimetric measurements. The four dosimeters flown on the RaD-X science payload are a Hawk version 3.0 tissue equivalent proportional counter (TEPC) manufactured by Far West Technologies [*Conroy*, 2010]; a Liulin dosimeter-spectrometer developed by the Solar Research and Technology Institute, Bulgarian Academy of Sciences [*Dachev et al.*, 2015]; a total ionizing dose (TID) detector manufactured by Teledyne Microelectronic

Technologies [*Mazur et al.*, 2011]; and the RaySure detector provided by the University of Surrey [*Hands and Dyer*, 2009]. The energy deposition spectra measured by the TEPC and Liulin instruments are used to characterize the contributions of cosmic ray primaries to the dosimetric measurements. The TID and RaySure detectors are potential technologies for the development of a distributed network of real-time measurements of the aircraft cosmic radiation environment.

Significant scientific enhancements to the RaD-X balloon flight were provided by supporting aircraft measurements that were nearly spatially temporally coincident with the balloon trajectory. The NASA Armstrong Flight Research Center ER-2 aircraft, equipped with a TEPC instrument by the Upper-atmospheric Space and Earth Weather eXperiment (USEWX) project, took dosimetric measurements at an altitude of 20 km near the Pfotzer maximum, corresponding to the peak in secondary particle production, and at an altitude of 17 km just below the Pfotzer maximum where attenuation processes dominate over production processes. DLR conducted a flight campaign on 12 and 15 September 2015 at geomagnetic vertical cutoff rigidities similar to the RaD-X balloon flight (~4 GV). The DLR campaign composed of two Lufthansa German Airline commercial flights equipped with TEPC and Liulin instruments, with cruise altitudes between ~10 and 11 km. TEPC and Liulin instruments flown on a Cessna Conquest II aircraft, operated by Columbia Scientific Balloon Facility at Fort Sumner, NM, provided dosimetric measurements at 8 km, which is the low range of commercial aircraft cruising altitudes. In total, the RaD-X mission provided dosimetric measurements at seven key altitudes that are important for characterizing and assessing the physics of aviation radiation exposure.

3. Dosimetric Quantities

The dosimetric quantities used in human radiation protection applications are defined and briefly described in this section. A fundamental dosimetric quantity in radiological protection is absorbed dose. Absorbed dose is defined as the energy deposited per mass in a target medium by the radiation field. The SI unit for absorbed dose is the Gray (1 Gy = J/kg).

Absorbed dose alone is not an indicator of the severity of biological damage to a tissue cell, however. The relative effectiveness in producing biological damage depends not only on absorbed dose but also on the type of particle and energy of the particle producing the dose. This is accounted for by weighting the tissue-averaged absorbed dose by a factor related to the quality of the radiation. Equivalent dose is the name given by the ICRP for the radiation quality-weighted tissue-averaged absorbed dose *International Commission on Radiological Protection (ICRP)* [2007]. The SI unit of equivalent dose is the Sievert (Sv). Thus, equivalent dose in tissue T from particle j is denoted $H_{j,T}$, which is given in terms of the radiation weighting factor w_j and the tissue-averaged absorbed dose from particle j, denoted $D_{j,T}$, such that

$$H_{j,T} = w_j D_{j,T}. \tag{1}$$

The radiation weighting factor is a function of energy for neutrons [*International Commission on Radiological Protection (ICRP)*, 2007].

The probability of biological damage also depends on the specific organ or tissue irradiated. The relative contributions of each organ or tissue to the total biological detriment to the human body caused by the radiation field is incorporated into the dosimetric quantity referred to as the effective dose. Denoted E, effective dose is defined as the weighted sum of equivalent dose over all the tissues and organs in the human body, such that

$$E = \sum_T \sum_j w_T H_{j,T}. \tag{2}$$

The organ and tissue weighting factors are also given in the ICRP report [*International Commission on Radiological Protection (ICRP)*, 2007].

The recommended ICRP radiation exposure limits and guidelines are expressed in terms of effective dose. However, effective dose is not a practical quantity to measure. Ambient dose equivalent is an operational quantity introduced by the ICRP/ICRU for radiation protection applications, which is denoted by $H^*(d)$ [*International Commission on Radiological Protection (ICRP)*, 2007; *ICRU*, 2010]. Conceptually, $H^*(d)$ refers to the dose equivalent that would be produced by the corresponding expanded and aligned field at a depth d in millimeters along the radius vector of a 300 mm diameter spherical tissue-equivalent phantom material (the so-called ICRU sphere) opposing the direction of the aligned field. The quantity recommended for use as a reasonable operational proxy for effective dose is $H^*(10)$, the ambient dose equivalent at a depth of 10 mm.

Ambient dose equivalent is defined above in terms of dose equivalent, which is not the same as the equivalent dose in (1). Equivalent dose is defined as the product of a tissue-averaged or organ-averaged absorbed dose multiplied by a discrete radiation weighting factor. On the other hand, dose equivalent is defined at a point **x** in the target medium and is computed in terms of a continuous radiation quality factor. Explicitly, the dose equivalent at position **x** in tissue T from particle j is defined by

$$H_{j,T}(\mathbf{x}) = \int_L Q(L) D_{j,T}(\mathbf{x}, L) \mathrm{d}L, \tag{3}$$

where $H_{j,T}(\mathbf{x})$ and L denote dose equivalent and unrestricted linear energy transfer (LET), respectively, $D_{j,T}(\mathbf{x}, L)$ is the LET-spectral dose distribution, and $Q(L)$ is the tissue LET-dependent quality factor [*International Commission on Radiological Protection (ICRP)*, 2007]. Ambient dose equivalent, $H^*(10)$, can be computed from (3); it is the dose equivalent that would be produced by the corresponding expanded radiation field in the ICRU sphere at a depth of 10 mm along the radius vector opposing the direction of the aligned field, summed over all particles in the radiation field and summed over all tissues and organs in the human body (i.e., sum over all j and T in (3)).

One advantageous feature of dose equivalent and ambient dose equivalent is that microdosimeter measurements can be used to obtain these quantities. Microdosimeters can derive dose equivalent in tissue by combining the quality factor $Q(L)$ with a measurement of the LET-spectral dose distribution in a tissue-equivalent material, according to (3). Microdosimeters can also be calibrated to infer $H^*(10)$ [*Lillhök et al.*, 2007; *Silari et al.*, 2009; *ICRU*, 2010]. This is an important capability in radiation environment monitoring since $H^*(10)$ is an acceptable approximation for effective dose [*Meier et al.*, 2009; *ICRU*, 2010].

An important assumption implicit in (3) is that lineal energy (y) is approximated by the unrestricted LET (L). Lineal energy is the relevant microdosimetry quantity, which is the energy deposited in a volume of target medium per average chord length of the target volume [*ICRU*, 1983]. Unrestricted LET is the energy lost by an ionizing particle to the target medium per unit distance, which can overestimate the lineal energy under certain conditions. Model calculations commonly approximate lineal energy by LET, which is equated to the stopping power [*Wilson et al.*, 1991]. While the measured spectrum of the TEPC is routinely referred to as the LET spectrum [*Conroy*, 2010; *Mertens et al.*, 2016], in actuality it is the more accurate and relevant lineal energy spectrum [*ICRU*, 1983; *Straume et al.*, 2016].

The dosimetric quantities measured during the RaD-X campaign are absorbed dose in tissue (TEPC) and in silicon (Liulin, TID, and RaySure), dose equivalent (TEPC and RaySure), $H^*(10)$ (TEPC), LET-spectral dose distribution in tissue (TEPC), and energy deposition spectra in silicon (Liulin and RaySure). A more detailed description of the RaD-X instruments is given by *Straume et al.* [2016]. The complete list of dosimetric quantities obtained by each instrument that contributed to the RaD-X campaign is given in Tables 1 and 2 by *Mertens et al.* [2016].

4. Summary of RaD-X Special Issue Articles

This section gives a brief summary of the articles that comprise the RaD-X special issue of space weather, highlighting the interdependencies among eight additional papers and the contributions that each article makes to the science goals of the RaD-X mission.

The paper by *Straume et al.* [2016] presents results of prelaunch exposure of the RaD-X instruments (TEPC, Liulin, TID, and RaySure) to known (National Institute of Standards and Technology (NIST) traceable) Co-60 and Cf-252 radiation sources at Lawrence Livermore National Laboratory (LLNL). These standard, NIST-traceable measurements were used to calibrate the two RaD-X TEPCs: the balloon flight instrument and the flight spare. For absorbed dose rate measurement comparisons between the RaD-X instruments and the LLNL Co-60 gamma ray standard, the dosimeter-to-standard measurement ratios were 0.84 ± 0.06, 1.07 ± 0.32, 1.31 ± 0.07, and 0.82 ± 0.24 for the TEPC, TID, Liulin, and RaySure, respectively. These comparisons were used to estimate the systematic uncertainty of the flight-averaged absorbed dose rate measurements taken during the RaD-X balloon flight [*Mertens et al.*, 2016]. Moreover, the dosimeter-to-standard measurement ratios aided the interpretation of the intercomparisons of the RaD-X instrument flight measurements. The prelaunch ground tests also included RaD-X instrument comparisons to the LLNL Cf-252 fission source, which emits both neutron and gamma ray radiations. In this case, the dosimeter-to-standard measurement ratios were 0.94 ± 0.15,

0.55 ± 0.18, 0.58 ± 0.08, and 0.32 ± 0.12, respectively, for the TEPC, TID, Liulin, and RaySure. The silicon-based dosimeters significantly underresponded to the Cf-252 radiation source, which is discussed in *Straume et al.* [2016].

The paper by *Gronoff et al.* [2016] derives payload structure correction factors that are applied to the flight measurements [*Mertens et al.*, 2016]. The TEPC instrument is housed in a pressurized aluminum container. All the science instruments are mounted to an aluminum structure and thermally protected by a foam cover. The payload structure not only partially attenuates the ambient cosmic radiation but also creates secondary radiations via collisional interactions between the incident cosmic radiation and the payload structure material. Thus, the payload structure modifies the ambient radiation environment observed by the instruments. The influence of the payload structure on the measured dosimetric quantities is estimated using model simulations. Specifically, a detailed computer-aided design model of the RaD-X payload structure, combined with comprehensive radiation environment modeling using the Geant4 Monte Carlo transport code [*Desorgher et al.*, 2005; *Agostinelli et al.*, 2003], is utilized to derive payload structure correction factors that are applied to the RaD-X instrument dosimetric measurements. The correction factors are derived for the individual RaD-X science instruments as a function of depth within the atmosphere. Overall, the payload structure modifies the ambient cosmic radiation environment by no more than 7% in terms of the measured dosimetric quantities.

The paper by *Mertens et al.* [2016] presents measurement results from both the RaD-X balloon flight and the supporting aircraft flights. A detailed description of the flight campaign is given. The RaD-X flight mission provided benchmark, flight-averaged dosimetric measurements at seven altitudes from 8 km to over 32 km. The conservatively estimated total uncertainty of the benchmark flight measurements is less than the 30% ICRU/ICRP criterion for dose assessments [*ICRU*, 2010]. Furthermore, to our knowledge, the RaD-X TEPC and Liulin spectral dose distribution measurements are the first published at these altitudes. The flight-averaged dosimetric quantities, combined with the spectral dose distribution measurements, provide an important data set for improving the understanding of cosmic radiation transport in the atmosphere and human exposure to atmospheric ionizing radiation in the aircraft environment. The TEPC, Liulin, and TID measurements agreed to within 15% with respect to the flight-averaged absorbed dose rates, which is less than the estimated total uncertainty of the measurements. The outcome of the instrument intercomparisons strengthens the case for using the TID to monitor the atmospheric ionizing radiation environment. The advantages and disadvantages of both the RaySure and TID technologies are discussed with respect to real-time aviation radiation measurements.

The details of the RaySure measurements taken during the RaD-X balloon flight are discussed by *Hands et al.* [2016]. By comparing altitude profiles of dose equivalent rate, the RaySure differs from the TEPC measurements by no more than 25%. Both the RaySure and TEPC instruments observed an absence of a distinct Pfotzer maximum in the dose equivalent rate. Previous balloon measurements showed a peak in dose equivalent rate at the altitude of the Pfotzer maximum, which was an artifact of the limited LET range of these dosimeters. Thus, the absence of a peak in dose equivalent rate observed by the RaySure and TEPC is an indication that the RaD-X mission provided an improvement in high-altitude dosimetric measurements. The general good agreement between the RaySure and TEPC shows that the original RaySure calibration factors for deriving dose equivalent rate from the count rate spectrum are fairly robust. However, analysis of the RaySure data during the RaD-X ground tests and flight measurements, along with previous measurements in the aircraft radiation environment, has shown a fairly large spread in measurements of the tissue-to-silicon-absorbed dose rate ratio, which dominates the uncertainty in determining dose equivalent rate from the measurements of the RaySure count spectrum. Additional laboratory and flight campaigns are needed to better quantify this ratio in different radiation environments and reduce its uncertainty. Nevertheless, the overall performance of the RaySure during the RaD-X balloon flight shows that this instrument remains a viable technology for continuous monitoring of human exposure in the aviation radiation environment.

The paper by *Meier et al.* [2016] presents the results of the DLR flight campaign in support of the RaD-X mission. The DLR campaign consisted of a round-trip Lufthansa German Airline commercial flight from Germany to Japan. This flight route was selected because the flight-averaged geomagnetic vertical cutoff rigidity is similar to the RaD-X balloon flight. The average cruise altitudes were 10.4 km and 11.3 km. The Lufthansa aircraft was equipped with a TEPC and a Liulin. Flight-averaged absorbed dose rates in silicon were obtained from the Liulin measurements, and $H^*(10)$ rates were derived from the TEPC measurements. These results were

also compared to the NAIRAS and PANDOCA models. The flight-averaged dosimetric quantities were reported with the other supporting aircraft measurements in the RaD-X flight paper [*Mertens et al.*, 2016].

The paper by *Tobiska et al.* [2016] presents TID measurements from extensive aircraft flight data conducted by the Automated Radiation Measurements for Aerospace Safety (ARMAS) project. TID flight measurements have been collected from 184 flights on various research aircraft. The flights occurred during a variety of space weather conditions over a 3 year period and have covered low, middle, and high latitudes with altitudes reaching over 17 km. The novelty of the ARMAS system, based on the TID detector, is that the measurements are transmitted to the ground in real time and used by the NAIRAS model to adjust the prediction of radiation exposure along the aircraft flight path. This achievement is a major milestone toward improving physics-based global atmospheric ionizing radiation model predictions using the assimilation of real-time measurement data. One of main disadvantages of using the TID for monitoring the aircraft radiation environment is that the TID detector does not directly measure the radiological dosimetric quantities related to health risk (i.e., dose equivalent or $H^*(10)$). However, the results of this paper show that this deficiency may be mitigated by the development of an empirical calibration curve for calculating $H^*(10)$ using the TID measurements of the absorbed dose rate in silicon.

The paper by *Norman et al.* [2016] compares dose rate calculations with the RaD-X balloon flight measurements. The model calculations used the HZETRN transport code with three different GCR models, which specify the cosmic ray primary flux spectra at 1 AU (astronomical unit) outside the magnetosphere. The purpose of the model comparisons is to test GCR models that are widely used in specifying the input radiation environment in aviation radiation models. It was shown that the largest differences in cosmic ray flux spectra among the three GCR models were at energies where transmission through the magnetosphere was nearly zero in the vicinity of Fort Sumner, NM, due to the ~4 GV geomagnetic vertical cutoff rigidity. Thus, the calculated dosimetric quantities were roughly the same using the three GCR models. The model calculations of absorbed dose rates in tissue agreed well with the RaD-X balloon flight TEPC measurements. The model calculations of absorbed dose rate in silicon underpredicted the Liulin measurements by about 30%, which may be a consequence of the overresponse of the Liulin instrument observed in the laboratory exposures [*Straume et al.*, 2016]. However, the model calculations of dose equivalent rate were significantly larger than the TEPC measurements. Furthermore, the influence of heavy-ion cosmic ray primaries is clearly discernable in the model calculations of dose equivalent rate and the average quality factor. On the other hand, evidence of heavy-ion contributions in the measured dose equivalent rate is inconclusive. The larger mix of high-LET radiations in the model calculations of dose equivalent rate and average quality factor may be an artifact of the 1-D transport calculations, among other things. Future modeling work will include the contributions of the off-axis (i.e., nonvertical) rays, along with detailed comparisons with the TEPC and Liulin spectral dose distribution measurements, as the integrated (dose rates) quantities alone were shown to be insufficient to understand the sources of discrepancies between model calculations and the measurements.

The paper by *Phillips et al.* [2016] presents dose rates measured from stratospheric weather balloons near Bishop, California. The balloon launches were conducted by the student-led "Earth to Sky Calculus" organization. The science payloads consist of affordable technologies that are accessible to high schools and small colleges. The dose rates were measured by a detector sensitive to X-rays and gamma rays. The results shown in this paper complement the dosimetric measurements taken during the RaD-X flight campaign by showing the variation in dose rates at the Pfotzer maximum at a location near Fort Sumner, NM, during various space weather events, such as the arrival of a coronal mass ejection, a Forbush decrease, and a geomagnetic storm.

5. Conclusions

The RaD-X balloon flight provided measurements from four different type dosimeters at a high-altitude region where measurement data are sparse. The dosimetric balloon measurements above the Pfotzer maximum are influenced by cosmic ray primaries, which are the ultimate source of radiation exposure at aircraft altitudes. The altitudes of the supporting aircraft flights were selected to correspond to regions in the atmosphere where the cosmic radiation transport and collisional interaction physics are characteristically distinct from one another. The flight times at constant float altitudes and geomagnetic vertical cutoff rigidity enabled a significant reduction in the statistical uncertainty of the dosimetric measurements. The vertical cutoff rigidity of the flight measurements corresponds to a value where aviation radiation model uncertainty is near its peak of ~50% [*Bottollier-Depois et al.*, 2012], including the NAIRAS model [*Mertens et al.*, 2013]. The total

standard uncertainty of the flight-averaged dosimetric quantities at the seven RaD-X flight altitudes is less than the ICRU/ICRP criterion of 30% for dose assessments [*ICRU*, 2010]. As a result, the RaD-X measurements, in principle, can lead to nearly a factor of 2 reduction in the prediction of the radiation protection quantities in the region of maximum model uncertainty. Consequently, the mission summary above indicates that the high-quality RaD-X flight-averaged dosimetric quantities will provide an important data set for improving the understanding of cosmic radiation transport and human exposure to ionizing radiation in the aircraft environment, which is the first goal of the RaD-X mission.

The initial model comparisons to the RaD-X balloon flight measurements by *Norman et al.* [2016] provide the impetus to make a few general remarks concerning the source(s) of aviation radiation model uncertainty. Differences among the widely available GCR models cannot explain the systematic underprediction of aviation radiation models at low latitudes and high-geomagnetic vertical cutoff rigidities [*Bottollier-Depois et al.*, 2012; *Mertens et al.*, 2013], as the GCR model differences are largely confined to energies below the vertical cutoff rigidity of the RaD-X flights [*Norman et al.*, 2016]. As a result, high-latitude and low-geomagnetic vertical cutoff rigidity balloon flights are needed to select a preferred GCR model for aviation radiation exposure applications. Moreover, future V&V work will entail a comparison of GCR model cosmic ray primary proton flux spectrum with the recent Alpha Magnetic Spectrometer measurements on the International Space Station [*Aguilar et al.*, 2015], to assess whether or not there is a systemic underprediction of primary protons in the 4 GV to 20 GV rigidity range common to all the available GCR models. Furthermore, vertical cutoff rigidity itself is no longer a unique quantity at middle to low latitudes due to the penumbra effect [*Smart and Shea*, 2003]; in addition, the directional dependence of the cutoff rigidity becomes more important at midlatitude to low latitude [*Badavi et al.*, 2011]. Therefore, the assumptions used in aviation radiation models to specify the geomagnetic transmission of cosmic radiation through the geomagnetic field should be thoroughly examined. Moreover, a source of model uncertainty could also be related to the fundamental interaction cross sections and transport physics. For example, the physics of pion-initiated electromagnetic cascade processes is a possible domain of model uncertainty since these processes are relatively more important at low latitudes [*Mertens et al.*, 2013]. The potential sources of model uncertainty mentioned above, along with the influence of 1-D transport effects [*Norman et al.*, 2016], will be assessed using the RaD-X flight data in a future NAIRAS V&V effort.

The RaD-X balloon flight trajectory profile was designed to provide dosimetric quantities that are influenced by cosmic ray primaries. The larger flight-averaged dose equivalent rate and average quality factor in Region B compared to Region A is consistent with high-LET radiations from heavy-ion primaries in Region B [*Norman et al.*, 2016]. However, when measurement uncertainty is included, the differences between the integrated (dose rate) dosimetric measurements in Regions A and B are within the uncertainty estimates. However, the TEPC and Liulin spectral dose distribution measurements show distinctly different energy deposition characteristics between Regions A and B. The spectral measurements provide observations of the complex mixture of high-LET and low-LET radiations above the Pfotzer maximum. These measurements are valuable in assessing model specification of cosmic ray primaries, from both light ions and heavy ions, and backscattered neutrons and low-LET charged particles produced near the region of the Pfotzer maximum. The future NAIRAS V&V effort will also include comparisons to the RaD-X spectral measurements. To our knowledge, the paper by *Mertens et al.* [2016] is the first to publish TEPC and Liulin spectral dose measurements in the stratosphere.

The second goal of the RaD-X mission is to identify and characterize low-cost, compact radiation detectors for application to long-term, continuous monitoring of the aircraft radiation environment. The two candidate technologies selected to address this goal were the RaySure and TID, as the analysis of the measurements obtained from these detectors represent very different approaches to monitoring human exposure to cosmic radiation. The RaySure measures the energy deposition spectrum of the ionizing radiation field in silicon, which enables the radiological quantities related to health risk to be calculated from the measured spectrum, using appropriate calibration factors. This is one of the main advantages of the RaySure detector. RaySure measurements of dose equivalent rate agree very well with TEPC measurements in the aircraft environment [*Hands and Dyer*, 2009], and the agreement was generally good at the RaD-X balloon flight altitudes [*Hands et al.*, 2016]. The main disadvantage is that there are only a few units available, units which have been built for research applications. By contrast, the manufacturing production of the TID is make-to-order through Teledyne Microelectronic Technologies. Nevertheless, there are two main disadvantages to using the TID detector for monitoring aviation radiation exposure. First, the TID measures total absorbed dose, which requires an extensive in-flight calibration procedure to develop an empirical fit of absorbed dose in silicon

to the radiological quantities relevant to human exposure. However, the ARMAS project is developing such a in-flight calibration procedure, and this approach appears promising [*Tobiska et al.*, 2016]. Second, precision dose rates are difficult to derive from the TID accumulated absorbed dose measurements in the low-intensity aircraft radiation environment. On the other hand, the analysis technique developed by *Mertens et al.* [2016] in processing the RaD-X TID flight data was successful in mitigating this issue. In short, both the RaySure and TID detectors performed well during the RaD-X balloon flight and remain viable candidates for real-time monitoring of the aircraft radiation environment. It is our opinion that both technologies should continue to be supported and advanced.

A number of outstanding issues were identified in the analysis of the RaD-X flight data, which argue for additional flight measurements and laboratory experiments. At minimum, these issues could be addressed by a flight campaign conducted at high-latitude and low-geomagnetic vertical cutoff rigidity. High-latitude measurements would provide a different radiation environment to better understand the unexpected low value of the measured absorbed dose rate in tissue to silicon observed at the RaD-X balloon flight altitudes [*Hands et al.*, 2016; *Mertens et al.*, 2016]. Furthermore, the flight measurements should be supplemented by laboratory experiments where the RaD-X instruments are exposed to high-LET and low-LET charged particle sources. Addressing the low value for the tissue-to-silicon absorbed dose rate ratio is also tied to understanding the difference between the RaySure and TEPC dose equivalent rate measurements above the Pfotzer maximum, which would likely lead to an improvement in the RaySure calibration. Flight measurements at low-vertical cutoff rigidity would provide dose and spectral measurements with a different mixture of high-LET and low-LET radiations, enhancing the measurement data available for aviation radiation model improvement. Moreover, high-latitude flight measurements are better suited for quantifying the performance of the widely accessible GCR models for application to aviation radiation exposure prediction [*Norman et al.*, 2016]. Since the GCR models are each fit to different data sets using various transport codes, the balloon flight measurements would be useful as an independent data set for testing the GCR models for space radiation applications as well. Another valuable feature of the RaD-X mission is that the science payload can be flown on future balloon missions or dedicated aircraft campaigns with minimal development cost.

Acknowledgments

The RaD-X mission was funded by the NASA Science Mission Directorate under the Hands-On Project Experience (HOPE)-4 opportunity. Civil Servant labor costs were provided by NASA Langley Research Center (LaRC), NASA Ames Research Center, and NASA Wallops Flight Facility. LaRC also contributed to facility costs, science instrument procurements (Science Directorate), and media and outreach costs. Lawrence Livermore National Laboratory provided their facility for radiation source exposure and calibration of the science instruments. Bryn Jones from SolarMetrics (United Kingdom) provided the TEPC instrument which flew on the NASA Armstrong Flight Research Center's ER-2 aircraft. The TEPC/ER-2 integration and testing were performed under the auspicies of the Upper-atmospheric Space and Earth Weather eXperiment (USEWX) project. Eric Benton at Oklahoma State University provided TEPC and Liulin instruments for flight on the Cessna Conquest II aircraft. Columbia Scientific Balloon Facility provided their Cessna aircraft for a dedicated flight to support the RaD-X mission.

References

Agostinelli, S., et al. (2003), Geant4—A simulations toolkit, *Nucl. Instr. Method Phys. Res. A*, *506*, 250–303.

Aguilar, M., et al. (2015), Precision measurement of the proton flux in primary cosmic rays from rigidity 1 GV to 1.8 TV with the Alpha Magnetic Spectrometer on the International Space Station, *Phys. Rev. Lett.*, *114*, 171103.

AMS (2007), Integrating space weather observations and forecasts into aviation operations, Tech. Rep., Am. Meteorol. Soc. Policy Program and SolarMetrics, Washington, D. C.

Aspholm, R., M.-L. Lindbohm, H. Paakkulainen, H. Taskinen, T. Nurminen, and A. Tiitinen (1999), Spontaneous abortions among Finnish flight attendants, *J. Occupational Environ. Med.*, *41*(6), 486–491.

Badavi, F. F., J. E. Nealy, and J. W. Wilson (2011), The low earth orbit validation of a dynamic and anisotropic trapped radiation model through ISS measurements, *Adv. Space Res.*, *48*, 1441–1458, doi:10.1016/j.asr.2011.06.009.

Bazilevskaya, G. A. (2000), Observations of variability in cosmic rays, *Space Sci. Rev.*, *94*, 25–38.

Bazilevskaya, G. A., and A. K. Svirzhevskaya (1998), On the stratospheric measurements of cosmic rays, *Space Sci. Rev.*, *85*, 431–521.

Bennett, L. G. I., B. J. Lewis, B. H. Bennett, M. J. McCall, M. Bean, L. Doré, and I. L. Getley (2013), A survey of the cosmic radiation exposure of Air Canada pilots during maximum galactic radiation conditions in 2009, *Radiat. Meas.*, *49*, 103–108.

Bottollier-Depois, J. F., P. Beck, M. Latocha, V. Mares, D. Matthiä, W. Rühm, and F. Wissmann (2012), Comparison of codes assessing radiation exposure of aircraft crew due to galactic cosmic radiation, *EURADOSE Rep. 2012-03*, EURADOSE, Braunschweig, Germany.

Conroy, T. (2010), *Environmental Radiation Monitor with 5″ Tissue Equivalent Proportional Counter (TEPC), Hawk Version 3, Model FWAD-3*, Operations and Repair Manuel, Far West Technology, Goleta, Calif.

Copeland, K., H. H. Sauer, F. E. Duke, and W. Friedberg (2008), Cosmic radiation exposure on aircraft occupants on simulated high-latitude flights during solar proton events from 1 January 1986 through 1 January 2008, *Adv. Space Res.*, *42*, 1008–1029.

Copeland, K. A. (2014), Cosmic ray particles fluences in the atmosphere resulting from primary cosmic ray heavy ions and their resulting effects on dose rates to aircraft occupants as calculated with MCNPX 2.7.0, PhD thesis, Dep. of Chem. and Chem. Eng., Royal Military College of Canada, Kingston, Ont., Canada.

Dachev, T. P. (2013), Profile of the ionizing radiation exposure between the Earth surface and free space, *J. Atmos. Sol. Terr. Phys.*, *102*, 148–156.

Dachev, T. P., et al. (2015), Overview of the Liulin type instruments for space radiation measurement and their scientific results, *Life Sci. Space Res.*, *4*, 92–114.

Desorgher, L., E. O. Flückiger, M. R. Moser, and R. Bütikofer (2005), Atmocosmics: A GEANT4 code for computing the interaction of cosmic rays with the Earth's atmosphere, *Int. J. Mod. Phys. A*, *20*(29), 6802–6804, doi:10.1142/S0217751X05030132.

Dyer, C. S., F. Lei, S. N. Clucas, D. F. Smart, and M. A. Shea (2003), Calculations and observations of solar particle enhancements to the radiation environment at aircraft altitudes, *Adv. Space Res.*, *32*(1), 81–93.

Dyer, C., A. Hands, F. Lei, P. Truscott, K. A. Ryden, P. Morris, I. Getley, L. Bennett, B. Bennett, and B. Lewis (2009), Advances in measuring and modeling the atmospheric radiation environment, *IEEE Trans. Nucl. Sci.*, *56*(6), 3415–3422.

EURATOM (1996), Council Directive 96/29/EURATOM of 13 May 1996, Laying Down the Basic Safety Standards for Protection of the Health of Workers and the General Public Against the Dangers Arising from Ionising Radiation, *Official J. Eur. Communities*, *39*, L159.

Ferrari, A., M. Pelliccioni, and T. Rancati (1999), The role of the quantities used in radiobiological protection for the assessment of the exposure to cosmic radiation, *Radiat. Prot. Dosim.*, *88*(3), 199–210.
Fisher, G. (2009), Lessons from aviation: Linking space weather science to decision making, *Space Weather*, *7*, S03005, doi:10.1029/2008SW000432.
Friedberg, W., and K. Copeland (2011), *Ionizing Radiation in Earth's Atmosphere and in Space Near Earth*, DOT/FAA/AM-11/9, Office of Aerospace Medicine, Washington, D. C.
Gaisser, T. (1990), *Cosmic Rays and Particle Physics*, Cambridge Univ. Press, New York.
Getley, I. L. (2004), Observation of solar particle event on board a commcercial flight from Los Angeles to New York on 29 October 2003, *Space Weather*, *2*, S05002, doi:10.1029/2003SW000058.
Getley, I. L., M. L. Duldig, D. F. Smart, and M. A. Shea (2005), Radiation dose along North American transcontinental flight paths during quiescent and disturbed geomagnetic conditions, *Space Weather*, *3*, S01004, doi:10.1029/2004SW000110.
Grajewski, B., E. A. Whelan, C. C. Lawson, M. J. Hein, M. A. Waters, J. L. Anderson, L. A. MacDonald, C. J. Mertens, C-Y. Tseng, R. T. Cassinelli II, and L. Luo (2015), Miscarriage among flight attendants, *Epidemiology*, *26*(2), 192–203.
Gronoff, G. P., C. J. Mertens, R. B. Norman, T. C. Lusby, and T. Straume (2016), Assessment of the influence of the RaD-X balloon payload on the onboard radiation detectors, *Space Weather*, *14*, doi:10.1002/2016SW001405.
Hands, A., and C. Dyer (2009), A technique for measuring dose equivalent and neutron fluxes in radiation environments using silicon diodes, *IEEE Trans. Nucl. Sci.*, *56*(6), 3442–3449.
Hands, A., K. A. Ryden, and C. J. Mertens (2016), The disppearance of the Pfotzer-Regener maximum in dose equivalent measurements in the stratosphere, *Space Weather*, *14*, doi:10.1002/2016SW001402.
Hubiak, M. (2008), Experimentelle Bestimmung von Dosisraten auf Reiseflughoehen im solaren Minimum, diploma thesis, Fachhochschule Muenster University of Applied Sciences, Germany.
International Commission on Radiological Protection (ICRP) (1991), *ICRP Publication 60: 1990 Recommendations of the International Commission on Radiological Protection*, vol. 21(1–3), Pergamon Press, Oxford, U. K.
International Commission on Radiological Protection (ICRP) (2007), *ICRP Publication 103: The 2007 Recommendations of the International Commission on Radiological Protection*, vol. 37(2–4), Elsevier, Oxford, U. K.
ICRU (1983), International commission on radiation units and measurements, Microdosimetry, *ICRU Rep. 36*, Bethesda, Md.
ICRU (2010), International Commission on Radiation Units and Measurements, Reference data for the validation of doses from cosmic-radiation exposure of aircraft crew, ICRU Rep. 84,J. ICRU, 10(2), Oxford Univ. Press, Oxford, U. K.
Kataoka, R., T. Sato, and Y. Hiroshi (2011), Predicting radiation dose on aircraft from solar energetic particles, *Space Weather*, *9*, S08004, doi:10.1029/211SW000699.
Kress, B. T., C. J. Mertens, and M. Wiltberger (2010), Solar energetic particle cutoff variations during the 29–31 October 2003 geomagnetic storm, *Space Weather*, *8*, S05001, doi:10.1029/2009SW000488.
Lauria, L., T. J. Ballard, M. Caldora, C. Mazzanti, and A. Verdecchia (2006), Reproductive disorders and pregnancy outcomes among female flight attendants, *Aviation Space Environ. Med.*, *77*(7), 533–559.
Lillhök, J., et al. (2007), A comparison of ambient dose equivalent meters and dose calculations at constant flight conditions, *Radiat. Meas.*, *42*, 323–333.
Lindborg, L., D. T. Bartlett, P. Beck, I. McAulay, K. Schnuer, H. Straube, and F. Spurney (Eds.) (2004), Cosmic radiation exposure of aircraft crew. Compilation of measured and calculated data, Final Rep. of the EURADOS WG 5 to the Group of Experts established under Article 31 of the European Commission, Directorate-General for Energy and Transportation. Radiation Protection Issue No. 140, Luxembourg.
Mazur, J. E., W. R. Crain, M. D. Looper, D. J. Mabry, J. B. Blake, A. W. Case, M. J. Golightly, J. C. Kasper, and H. E. Spence (2011), New measurements of total ionizing dose in the lunar environment, *Space Weather*, *12*, S07002, doi:10.1029/2010SW000641.
Meier, M. M., D. Matthiä, T. Forkert, M. Wirtz, M. Scheibinger, R. Hübel, and C. J. Mertens (2016), RaD-X: Complementary measurements of dose rates at aviation altitudes, *Space Weather*, *14*, 689–694, doi:10.1002/2016SW001418.
Meier, M. M., M. Hubiak, D. Matthiä, M. Wirtz, and G. Reitz (2009), Dosimetry at aviation altitudes (2006–2008), *Radiat. Prot. Dosimetry*, *136*(4), 251–255.
Mertens, C. J., B. T. Kress, M. Wiltberger, S. R. Blattnig, T. S. Slaba, S. C. Solomon, and M. Engel (2010), Geomagnetic influence on aircraft radiation exposure during a solar energetic particle event in October 2003, *Space Weather*, *8*, S03006, doi:10.1029/2009SW000487.
Mertens, C. J., B. T. Kress, M. Wiltberger, W. K. Tobiska, B. Grajewski, and X. Xu (2012), Atmospheric ionizing radiation from galactic and solar cosmic rays, in *Current Topics in Ionizing Radiation Research*, edited by M. Nenoi, InTech Publisher.
Mertens, C. J., M. M. Meier, S. Brown, R. B. Norman, and X. Xu (2013), NAIRAS aircraft radiation model development, dose climatology, and initial validation, *Space Weather*, *11*, 603–635, doi:10.1002/swe.20100.
Mertens, C. J., et al. (2016), Cosmic radiation measurements from the RaD-X flight campaign, *Space Weather*, *14*, doi:10.1002/2016SW001407.
National Council on Radiation Protection and Measurements (2009), National council on radiation protection and measurements: Ionizing radiation exposure of the population of the United States, NCRP Rep. No. 160, National Council on Radiation Protection and Measurements.
Neher, H. V. (1967), Cosmic-ray particles that changed from 1954 to 1658 to 1965, *J. Geophys. Res.*, *72*(5), 1527–1539.
Norman, R. B., C. J. Mertens, and T. C. Slaba (2016), Evaluating galactic cosmic ray environment models using RaD-X flight data, *Space Weather*, *14*, doi:10.1002/2016SW001401.
Phillips, T., et al. (2016), Space weather ballooning, *Space Weather*, *14*, doi:10.1002/2016SW001410.
Reitz, G. (1993), Radiation environment in the stratosphere, *Radiat. Prot. Dosim.*, *48*(1), 5–20.
Singh, A. K., D. Siingh, and R. P. Singh (2011), Impact of galactic cosmic rays on Earth's atmosphere and health, *Atmos. Environ.*, *45*, 3806–3818, doi:10.1016/j.atmosenv.2011.04.027.
Silari, M., et al. (2009), Intercomparison of radiation protection devices in a high-energy stray neutron field. Part III: Instrument response, *Radiat. Meas.*, *44*, 673–691.
Smart, D. F., and M. A. Shea (2003), The limitations of using vertical cutoff rigidities determined from the IGRF magnetic field models for computing aircraft radiation dose, *Adv. Space Res.*, *32*(1), 95–102, doi:10.1016/S0273-1177(03)00501-5.
Spurný, F., K. Kudela, and T. Dachev (2004), Airplane radiation dose decrease during a strong Forbush decrease, *Space Weather*, *2*, S05001, doi:10.1029/2004SW000074.
Stassinopoulos, E. G., C. A. Stauffer, and G. J. Brucker (2003), A systematic global mapping of the radiation field at aviation altitudes, *Space Weather*, *1*(1), 1005, doi:10.1029/2003SW000011.
Straume, T., C. J. Mertens, T. C. Lusby, B. Gersey, W. K. Tobiska, R. B. Norman, G. P. Gronoff, and A. Hands (2016), Ground-based evaluation of dosimeters for NASA high-altitude balloon flight, *Space Weather*, *14*, doi:10.1002/2016SW001406.

Tobiska, W. K., et al. (2015), Advances in atmospheric radiation measurements and modeling needed to improve air safety, *Space Weather*, *13*, 202–210, doi:10.1002/2015SW001169.

Tobiska, W. K., et al. (2016), Global real-time dose measurements using the Automated Radiation Measurements for Aerospace Safety (ARMAS) system, *Space Weather*, doi:10.1002/2016SW001419.

United Nations Scientific Committee on the Effects of Atomic Radiation (2000), Sources and Effects of Ionizing Radiation, in *United Nations Scientific Committee on the Effects of Atomic Radiation UNSCEAR 2000 Report to the General Assembly, with Scientific Annexes*, vol. I: Sources, p. 647, United Nations, New York.

Waters, M., T. F. Bloom, and B. Grajewski (2000), The NIOSH/FAA working women's health study: Evaluation of the cosmic-radiation exposures of flight attendants, *Health Phys.*, *79*(5), 553–559.

Wilson, J. W., et al. (1991), Transport methods and interactions for space radiation, *NASA Tech. Rep. NASA-RP-1257*.

Wilson, J. W., I. W. Joes, D. L. Maiden, and P. Goldhagan (Eds.) (2003), Analysis, results, and lessons learned from the June 1997 ER-2 campaign, *NASA CP-2003-212155*, NASA Langley Research Center, Hampton, Va.

Wilson, J. W., C. J. Mertens, P. Goldhagan, W. Friedberg, G. D. Angelis, J. M. Clem, K. Copeland, and H. B. Bidasaria (2005), Atmospheric ionizing radiation and human exposure, *Tech. Rep. NASA/TP-2005-213935*, NASA, Washington, D. C.